VIP Lithium–Oxygen Battery | Very Important Paper

DOI: 10.1002/anie.201400711

Superior Rechargeability and Efficiency of Lithium–Oxygen Batteries: Hierarchical Air Electrode Architecture Combined with a Soluble Catalyst**

*Hee-Dae Lim, Hyelynn Song, Jinsoo Kim, Hyeokjo Gwon, Youngjoon Bae, Kyu-Young Park, Jihyun Hong, Haegyeom Kim, Taewoo Kim, Yong Hyup Kim, Xavier Lepró, Raquel Ovalle-Robles, Ray H. Baughman, and Kisuk Kang**

Abstract: *The lithium–oxygen battery has the potential to deliver extremely high energy densities; however, the practical use of Li-O_2 batteries has been restricted because of their poor cyclability and low energy efficiency. In this work, we report a novel Li-O_2 battery with high reversibility and good energy efficiency using a soluble catalyst combined with a hierarchical nanoporous air electrode. Through the porous three-dimensional network of the air electrode, not only lithium ions and oxygen but also soluble catalysts can be rapidly transported, enabling ultra-efficient electrode reactions and significantly enhanced catalytic activity. The novel Li-O_2 battery, combining an ideal air electrode and a soluble catalyst, can deliver a high reversible capacity (1000 mAh g^{-1}) up to 900 cycles with reduced polarization (about 0.25 V).*

Growing concerns over the depletion of fossil fuels and the environment has led to global efforts to secure sustainable energy supplies. One of the key elements to a sustainable energy solution is to develop long-life, efficient and low-cost energy storage systems. While Li-ion batteries have served as one of the most reliable energy storage systems thus far, Li-O_2 batteries have recently attracted a considerable amount of interest as an alternative to conventional Li-ion batteries. Li-O_2 chemistry theoretically delivers the greatest energy density among various types of batteries by eliminating the use of the heavy transition metals typically used as redox elements.[1–4] Li-O_2 batteries operate based on simple reaction chemistry between Li ions and oxygen ($2Li^+ + O_2 + 2e^- \rightarrow Li_2O_2$, $E^o = 2.96$ V vs. Li/Li^+).[5–8] The use of the unlimited source of oxygen as a cathode material is also a strong advantage for its possible widespread usage. Although the reaction mechanism is simple and straightforward, the practical use of Li-O_2 batteries has been restricted by their high over-charge potential, low energy efficiency, and poor cyclability.[9,10] These drawbacks are attributable to the formation of solid-type and nonconductive Li_2O_2 discharge products, which induce not only high polarization when they decompose during charging but also poor rate capability and poor reversibility. For these reasons, "rechargeable" Li-O_2 batteries cannot be operated over a certain number of cycles which is far less than that under which Li-ion batteries typically operate. Moreover, the energy efficiency (output energy/input energy) is unacceptably low for use as an energy storage system.[11,12]

To overcome the limitations of current Li-O_2 battery technology, diverse approaches combining multiple strategies are required. One of the important elemental technologies related to this involves the promotion of the catalytic activity during the charging reaction of Li_2O_2, which is critical to decrease the polarization and increase the reversibility.[13] Thus far, various types of oxides and metals have been tried as catalysts, showing some improvements.[14–16] However, in addition to their insufficient catalytic activity, the immobile nature of the interface between the catalysts and the discharge products (solid–solid interface) has also limited the catalytically active region to an area close to the interface.[17] This implies that the incorporation of the catalysts in the electrode requires a proper design considering the possible morphology of the discharge products and the air electrode shape. On the other hand, recently suggested soluble catalysts using redox mediators potentially exhibit better catalytic activity than their solid counterparts.[13,18] Unlike immobile solid catalysts, diffusible catalysts are far more likely to catalyze the decomposition of the solid

[*] H.-D. Lim, J. Kim, H. Gwon, Y. Bae, K.-Y. Park, J. Hong, H. Kim, Prof. K. Kang
Center for Nanoparticle Research Institute for Basic Science (IBS)
Department of Materials Science and Engineering
Research Institute of Advanced Materials (RIAM)
Seoul National University, Seoul 151-742 (Republic of Korea)
E-mail: matlgen1@snu.ac.kr

H. Song, T. Kim, Prof. Y. H. Kim
School of Mechanical and Aerospace Engineering
Institute of Advanced Aerospace Technology
Seoul National University, Seoul 151-742 (Republic of Korea)

X. Lepró, R. Ovalle-Robles, Prof. R. H. Baughman
Alan G. MacDiarmid NanoTech Institute
University of Texas at Dallas, Richardson, TX 75083-0688 (USA)

[**] This work was supported by a National Research Foundation of Korea Grant funded by the Korean Government (MEST) (grant number NRF-2009-0094219), and by the Research Center Program of IBS (Institute for Basic Science) in Korea. This work was also supported by the Korea Institute of Energy Technology Evaluation and Planning (KETEP) grant funded by the Korea government Ministry of Trade, Industry and Energy though the human resources development program (grant number 20124010203320) and the Energy Efficiency & Resources program (grant number 20132020000270). This work was also supported by the National Research Foundation of Korea (NRF) grant funded by the Korea government (MSIP) (grant numbers 2009-0083512 and 2013-000688).

Supporting information for this article is available on the WWW under http://dx.doi.org/10.1002/anie.201400711.

 © 2014 Wiley-VCH Verlag GmbH & Co. KGaA, Weinheim

discharge products. Soluble catalysts can even reach the interior of the air electrode and facilitate the decomposition of nonconductive discharge products, even when the products are electrically isolated. However, in order to maximize the activity of diffusible catalysts, a corresponding air electrode design should be considered simultaneously.[19–24] The air electrode architecture needs to provide an environment for the diffusible catalyst effortlessly to penetrate throughout the entire air electrode area. It should also be capable of yielding discharge products with a morphology best suited for recharging reactions by the type of catalyst used.

In this respect, we combined a hierarchically woven porous carbon nanotube (CNT) fibril air electrode with a highly active redox mediator as soluble catalyst in our Li-O_2 cell. Upon cycling, the Li_2O_2 discharge products were uniformly coated as a thin layer on the CNT fibril, which provided a high surface area on which the soluble catalysts can effectively react. A cross-woven CNT fibril sheet provided aligned macro- and microscale pores to facilitate the rapid transport of both the reaction ions and the catalysts without clogging even after a deep discharge process.[20,25] We report that this multiple optimization approach resulted in high rechargeability in a Li-O_2 battery with the highest energy efficiency. The significantly enhanced catalytic activity caused by the continuous "highway" for diffusing catalysts also led to reduced polarization (ca. 0.25 V) and stable cyclability that exceeded 900 cycles with 1000 mAh g^{-1}. The enhancement of the rechargeability and the efficiency reported here is expected to pave the way to the development of practically "rechargeable" Li-O_2 batteries.

Redox mediators as a diffusible catalyst in Li-O_2 batteries must conform to several conditions. 1) The redox potential (oxidation/reduction) of the mediator should be compatible with that of Li_2O_2 formation, that is, the oxidation potential needs to be slightly higher than the equilibrium potential of the Li_2O_2 formation. 2) The oxidized form of the redox mediator should be capable of efficiently decomposing Li_2O_2. 3) The redox mediator must not react with electrolyte solvents or the Li metal anode, and it should be highly dissolvable in the electrolyte. Considering the above requirements, we selected LiI as the soluble redox mediator for our Li-O_2 system because of its appropriate redox potential and stability in conventional organic electrolytes.[18,26] The expected redox mediator reaction is one in which iodide (I^-) ions are initially oxidized on the electrode surface to I_3^- or I_2 while charging. Subsequently, the oxidized reactors (I_3^- or I_2) chemically react with Li_2O_2, producing Li^+ and O_2 gas, with a reverse reaction into the initial iodide (I^-) ions.[18,26]

Combined with the LiI redox mediator, the air electrode framework was optimized to facilitate its transport through the electrode and maximize the catalytic activity. Our combined strategy is schematically illustrated in Figure 1. In a conventional carbon electrode using Ketjen black or Super P carbon, the overpotential during charge is generally high without a catalyst (see the red line in Figure 1). When a soluble catalyst is used, the overpotential is reduced, but it can still be appreciably high if the clogging of the pores inhibits the efficient transport of both the catalysts and the reaction products during the discharge process (the blue line in Figure 1). This situation is feasible when irregular carbon particles in a conventional air electrode are distributed in a disorderly manner. In such a case, the discharge products are randomly agglomerated and block the pores of the air electrode.[20,27,28] On the other hand, a hierarchically aligned porous air electrode framework can prohibit clogging by the discharge products. The presence of both micro- and nano-

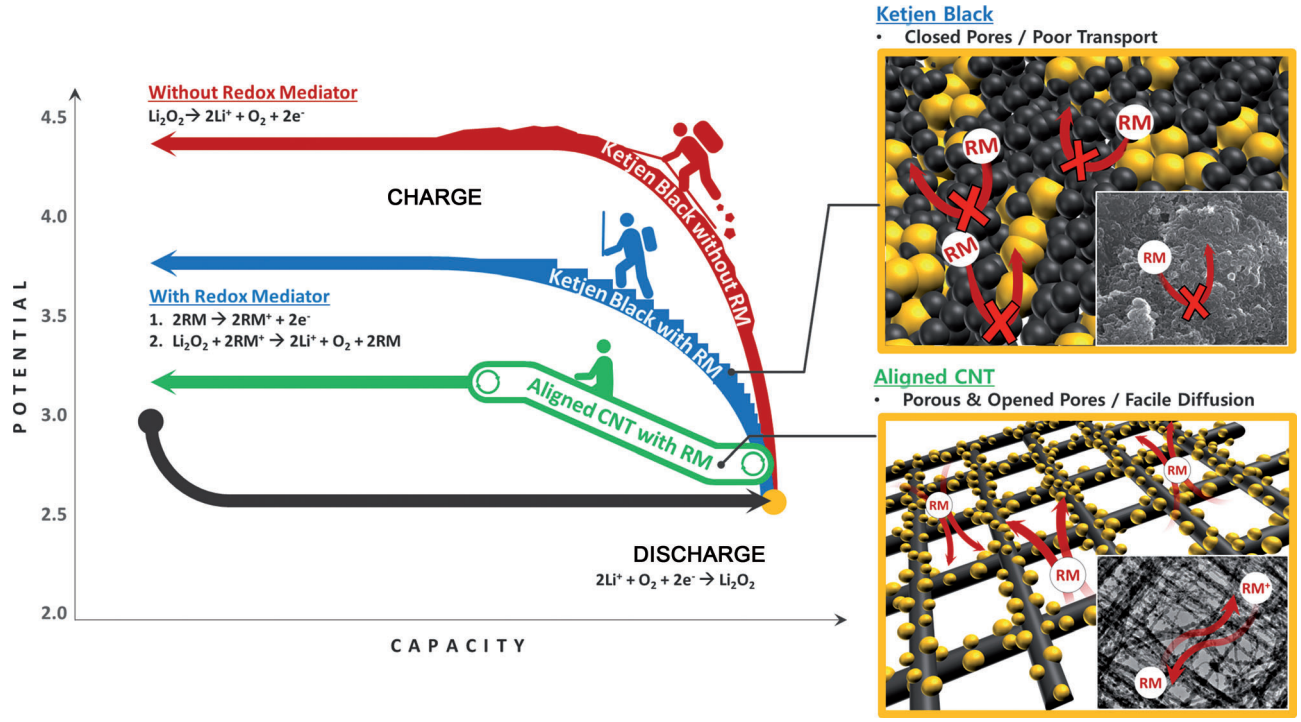

Figure 1. Schematic illustration of the role of the redox mediator (RM) in a Li-O_2 battery system made using a hierarchical CNT fibril electrode.

© 2014 Wiley-VCH Verlag GmbH & Co. KGaA, Weinheim

pores is expected to lead to a thin and uniform formation of Li_2O_2 on the CNT surface, which will maintain the rapid pathway for both the soluble catalyst and the reaction products (the green line in Figure 1).[20,25]

Figure 2 shows the electrochemical properties of CNT fibril electrodes with the LiI redox mediator. While CNT electrodes without catalysts exhibited a relatively high overpotential (ca. 1.5 V) during charge, a slightly lower overpotential (ca. 0.5 V) was observed in the presence of a solid Pt catalyst. Furthermore, an even lower overpotential (ca. 0.25 V) could be achieved with a soluble LiI catalyst. A marked reduction of the polarization was found regardless of the type of salt ($LiPF_6$ or LiTFSI) used, as shown in Figure 2a. The overpotential during charge is nearly identical to the theoretical reaction potential of I^- to I_3^- or I_2,[18,26] showing the smallest polarization value to date. The overpotential during charge is even lower than that during the discharge process. As a consequence of the reduction of the overpotential, the cyclability was dramatically improved, as shown in Figure 2b and c. Stable and reversible cycling was observed for more than 900 cycles without a notable change in the electrochemical profile. This cycle performance far exceeds those of the CNT fibril electrode without a catalyst (about 90 cycles)[20] or with Pt as a catalyst (about 170 cycles),[25] as shown in Figure S2 in the Supporting Information. Even when the discharge depth was increased to 3000 mA h g^{-1}, stable cycling was maintained for more than 300 cycles (Figure 2d).

The activity of the soluble redox mediator is believed to be synergistically enhanced through the combination with the hierarchically aligned porous CNT framework. Although Li-O_2 cells with a conventional carbon electrode (e.g., Ketjen black and binder) also showed reduced polarization when a soluble catalyst was used, as shown in Figure S3, they are greatly inferior compared to the aligned porous CNT fibril electrodes. The polarization during charge is still greater than 3.5 V and the enhancement of the cyclability is limited. These findings indicate that the performance of the redox mediator varies significantly depending on the structure of the air electrode, implying that an optimal environment for a soluble catalyst freely to diffuse through the interior/exterior of the air electrode is necessary to maximize the catalytic performance.

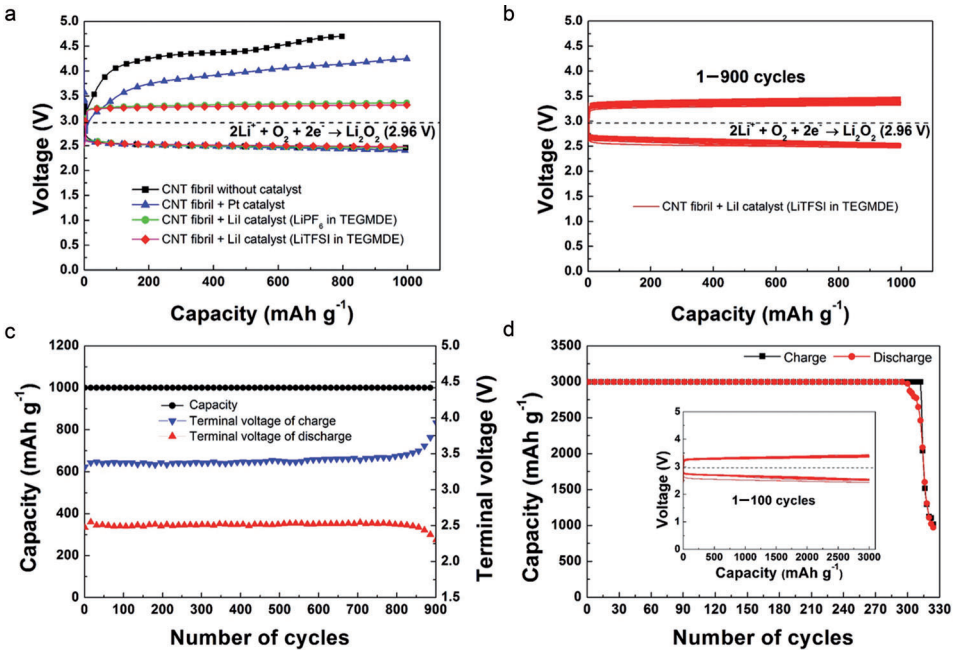

Figure 2. a) Discharge/charge profiles of CNT fibril electrodes without a catalyst, with the Pt catalyst, and with the LiI catalyst at a discharge depth of 1000 mA h g^{-1} and a current rate of 2000 mA g^{-1}. b) Electrochemical profiles and c) cyclability and terminal voltages of the CNT fibril electrodes with a LiI catalyst. d) Cyclability of the CNT fibril electrodes in the presence of a LiI catalyst at a discharge depth of 3000 mA h g^{-1}.

Along with the redox mediator and electrode architecture, another important aspect that we believe contributed to the cycle stability is the suppression of the side reactions that often take place with high-voltage cycling. The high charging voltage arising from the large polarization induces problems such as carbon corrosion and electrolyte deterioration.[29,30] Ottakam Thotiyl et al. showed that the irreversible formation of byproducts due to the corrosion of the carbon begins to occur above 3.5 V, resulting in poor cycle life of Li-O_2 batteries.[29] Byproducts including Li_2CO_3 and LiOH generally form during cycling and continuously accumulate on the carbon surface during this process. Decomposition of the tetraethylene glycol dimethyl ether (TEGDME) solvent is also triggered over 4.0 V, forming byproducts such as Li_2CO_3 and LiOH.[31,32] Given that the charge process is mainly done at 3.25 V and considering that the terminal voltage of the charge remains below 3.5 V (Figure 2c) during the cycling process, main side reactions are expected to be suppressed in our case.

The power capability of the Li-O_2 cell was tested at various current rates, as shown in Figure 3a and b. The current rate was gradually raised from 200 to 6000 mA g^{-1} and then reduced back to 200 mA g^{-1}. It is notable that the degree of polarization did not drastically increase, even when the current density was 30 times higher. The charging voltage remained below 3.5 V and the polarization did not exceed 0.5 V, even at the high current rate of 6000 mA g^{-1}. Furthermore, the electrochemical profiles remained nearly constant after the return to the initial rate, as shown in Figure 3b. This result demonstrates superior rate-capability and reversibility. For a further investigation of the reversibility of the Li-O_2 cells, the galvanostatic intermittent titration technique

 © 2014 Wiley-VCH Verlag GmbH & Co. KGaA, Weinheim

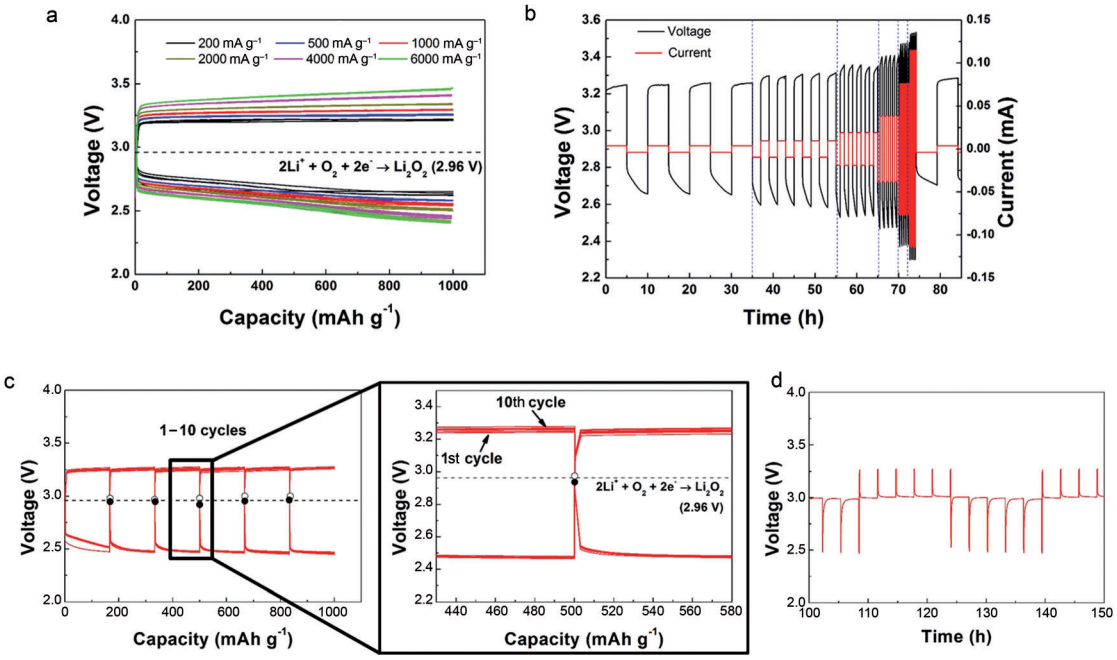

Figure 3. a,b) Power capability of CNT fibril electrodes in the presence of a LiI catalyst at current rates from 200 mA g^{-1} to 6000 mA g^{-1}. Each step is measured for five cycles. c) GITT voltage profiles and d) the corresponding potential versus time plot for 10 cycles. Three hours of relaxation time was allowed at each step.

(GITT) was used for ten consecutive cycles, as shown in Figure 3c and d. Nearly identical electrochemical profiles were observed for all cycles. The relaxation potential at each step approached the theoretical potential of Li_2O_2 formation, indicating that the formation/decomposition of Li_2O_2 continued quite reversibly.

The reversible formation/decomposition of Li_2O_2 was investigated further with a TEM analysis. Figure 4a shows that reaction products were deposited on the CNT surface after the discharge process. While most discharge products form a thin layer on the CNT, there were some bead-like products after the full discharge process. Nevertheless, they were dispersed on the CNT surface without clogging,[6,20,25,33] which is expected to provide a favorable environment for soluble catalysts efficiently to flow. The diffraction patterns in Figure 4c suggest the formation of Li_2O_2 during cycling. The observed bead formation and the diffraction patterns are consistent with previous reports in which no catalyst was used.[20,25] Upon charging, the Li_2O_2 completely disappear from the electrode, indicating high rechargeability, as shown in Figure 4b. The diffraction patterns in Figure 4c also confirm the absence of Li_2O_2 after the charge. Additionally, microscopic images of the formation/decomposition of Li_2O_2 were monitored by HR-TEM, as shown in Figure 4d. We observed that the Li_2O_2 begins to grow directly on the CNT surface with a thickness of a few nanometer until the half discharge. A slight modulation was detected for the thin Li_2O_2 layer on the CNT. With further lithiation, this modulation became more prominent and led to the formation of the bead-type particles. Charging of the air electrode reversed the reaction. The bead-type Li_2O_2 first disappears, and the modulated Li_2O_2 layer on the CNT then gradually fades away as the charge continues. Finally, all of the discharge products completely disappear at the end of the charging process.

The reversibility of the redox mediator was investigated by assessing whether the iodide ions (I^-) return to the initial state during cycling. Electrolytes in the as-prepared state, after discharging, and after charging were examined using Raman spectroscopy, as shown in Figure 4e. While the oxidized forms of I_2 and I_3^- have clear vibration modes at 189, 165, and 112 cm^{-1}, respectively, the initial form of I^- has no vibration mode.[34,35] No noticeable changes were observed after discharging and charging and no trace of I_2 or I_3^- ions was noted. These findings indicate that these oxidized species immediately return to their initial I^- ion state upon a reaction with Li_2O_2 during the charge process. To assess the ability of the redox mediator as catalysts further, we dissolved 0.05 M of I_2 in the TEGDME solvent and injected Li_2O_2 powder into the solvent. Figure 4f shows that oxygen gas evolved immediately after the injection of the Li_2O_2, indicating a rapid reaction between the redox mediator and the Li_2O_2. The volume of the evolved oxygen as measured by gas spectroscopy was about 4.14 mL, which is comparable to the expected value (4.48 mL) based on the reaction of $I_2 + Li_2O_2 \rightarrow 2Li^+ + 2I^- + O_2$.[18,26]

The combined approach using soluble catalysts and an aligned porous electrode can be applied to various types of Li-O_2 cells. As a model example, we applied this strategy to a hybrid Li-O_2 system in which dual electrolytes of TEGDME (liquid) and LiSICON (solid) were used in the configuration of Li metal anode/lithium bis(trifluoromethylsulfonyl)imide (LiTFSI) in the TEGDME/LiSICON/LiI + LiTFSI in TEGDME/cathode in sequence. Figure S4 shows that elec-

 © 2014 Wiley-VCH Verlag GmbH & Co. KGaA, Weinheim

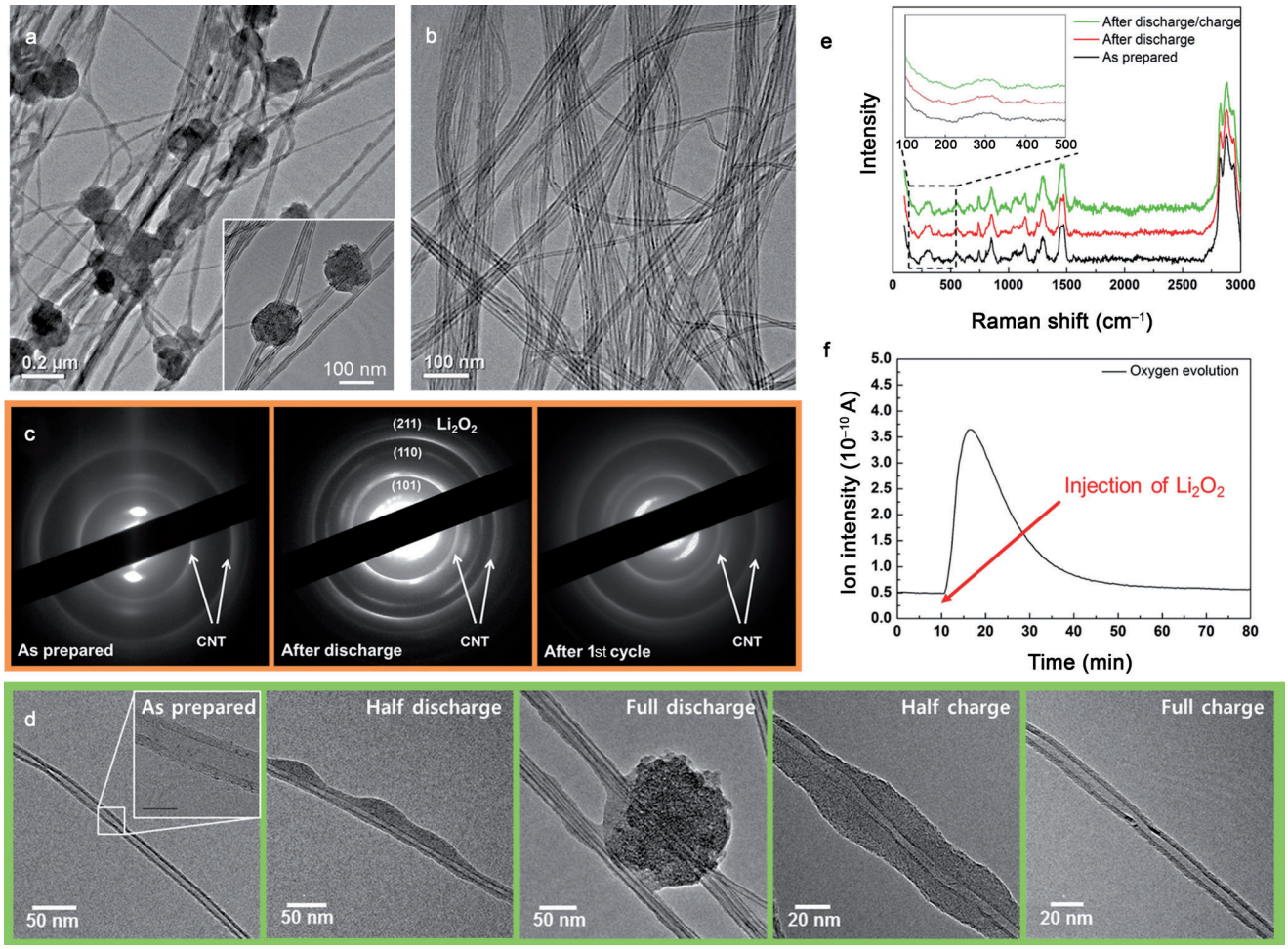

Figure 4. a,b) TEM images of the air electrode made using the LiI catalyst after the first discharge and first cycle. c) The corresponding diffraction patterns as prepared, post-discharge, and after the first cycle. d) Ex situ TEM analysis of the discharge products; the procedure for the formation of Li_2O_2 on the CNT surface and its decomposition (the scale bar in the left-hand inset is 10 nm). e) Raman spectra of the as prepared electrolytes, after the first discharge, and after the first cycle. f) Gas analysis of the evolved oxygen after injection of Li_2O_2 powder into 0.05 M I_2 dissolved in TEGDME solvent.

trochemical profiles analogous to the conventional Li-O_2 system were obtained in the hybrid Li-O_2 system with small overpotential levels, indicating that this combined approach is also valid in other types of Li-O_2 cells.

A persistent problem with all the current Li-O_2 cells, nevertheless, is that the electrolyte and Li metal is not sufficiently stable.[36–38] In the presence of Li metal, TEGDME forms LiOH byproducts on the Li anode;[13,36,37] thus, a protection layer on the anode is needed to prevent undesirable reactions. The partial formation of byproducts on the CNT surface also proceeds with cycles and eventually leads to cell failure. We found that the air electrodes after failure were covered with the byproducts of Li_2CO_3 and LiOH (Figure S5). The air electrode after failure could not be reused, even if we used a new electrolyte, separator, and Li metal. This implies that some degree of electrode degradation is unavoidable even if we control the degree of polarization below 3.5 V. The development of a reliably stable electrolyte and air electrode substrate is indispensable for even longer cycling exceeding 1000 times for Li-O_2 batteries. These problems must be addressed to spur further progress in Li-O_2 battery technology.

In summary, a highly efficient and reversible Li-O_2 battery was demonstrated using a hierarchically aligned porous air electrode in combination with a soluble LiI catalyst. The optimal design of the air electrode provides effectively rapid channels for both the reaction products and the soluble catalyst. The facile diffusion of the soluble catalyst throughout the entire air electrode could decrease the polarization during the charging process, enabling enhanced rechargeability and energy efficiency. The key challenge for future Li-O_2 batteries is synergistically to combine diverse elemental technologies for an overall performance enhancement.

Received: January 22, 2014
Published online: March 5, 2014

Keywords: catalysts · carbon nanotubes · lithium–oxygen battery · redox mediators

 © 2014 Wiley-VCH Verlag GmbH & Co. KGaA, Weinheim

[1] K. M. Abraham, Z. Jiang, *J. Electrochem. Soc.* **1996**, *143*, 1 – 5.
[2] P. G. Bruce, S. A. Freunberger, L. J. Hardwick, J.-M. Tarascon, *Nat. Mater.* **2012**, *11*, 19 – 29.
[3] D. Oh, J. Qi, Y.-C. Lu, Y. Zhang, Y. Shao-Horn, A. M. Belcher, *Nat. Commun.* **2013**, *4*, 2756.
[4] D. Zhai, H.-H. Wang, J. Yang, K. C. Lau, K. Li, K. Amine, L. A. Curtiss, *J. Am. Chem. Soc.* **2013**, *135*, 15364 – 15372.
[5] J.-J. Xu, Z.-L. Wang, D. Xu, L.-L. Zhang, X.-B. Zhang, *Nat. Commun.* **2013**, *4*, 2438.
[6] E. Yilmaz, C. Yogi, K. Yamanaka, T. Ohta, H. R. Byon, *Nano Lett.* **2013**, *13*, 4679 – 4684.
[7] H.-K. Lim, H.-D. Lim, K.-Y. Park, D.-H. Seo, H. Gwon, J. Hong, W. A. Goddard, H. Kim, K. Kang, *J. Am. Chem. Soc.* **2013**, *135*, 9733 – 9742.
[8] X. Ren, S. S. Zhang, D. T. Tran, J. Read, *J. Mater. Chem.* **2011**, *21*, 10118 – 10125.
[9] B. Sun, P. Munroe, G. Wang, *Sci. Rep.* **2013**, *3*, 2247.
[10] J. Lu, Y. Lei, K. C. Lau, X. Luo, P. Du, J. Wen, R. S. Assary, U. Das, D. J. Miller, J. W. Elam, H. M. Albishri, D. A. El-Hady, Y.-K. Sun, L. A. Curtiss, K. Amine, *Nat. Commun.* **2013**, *4*, 2383.
[11] S. Kumar, C. Selvaraj, N. Munichandraiah, L. G. Scanlon, *RSC Adv.* **2013**, *3*, 21706 – 21714.
[12] J.-L. Shui, H.-H. Wang, D.-J. Liu, *Electrochem. Commun.* **2013**, *34*, 45 – 47.
[13] Y. Chen, S. A. Freunberger, Z. Peng, O. Fontaine, P. G. Bruce, *Nat. Chem.* **2013**, *5*, 489 – 494.
[14] Y.-C. Lu, Z. Xu, H. A. Gasteiger, S. Chen, K. Hamad-Schifferli, Y. Shao-Horn, *J. Am. Chem. Soc.* **2010**, *132*, 12170 – 12171.
[15] Y. Lu, Z. Wen, J. Jin, Y. Cui, M. Wu, S. Sun, *J. Solid State Electrochem.* **2012**, *16*, 1863 – 1868.
[16] W.-H. Ryu, T.-H. Yoon, S. H. Song, S. Jeon, Y.-J. Park, I.-D. Kim, *Nano Lett.* **2013**, *13*, 4190 – 4197.
[17] H.-D. Lim, H. Gwon, H. Kim, S.-W. Kim, T. Yoon, J. W. Choi, S. M. Oh, K. Kang, *Electrochim. Acta* **2013**, *90*, 63 – 70.
[18] T. Shiga, Y. Hase, Y. Kato, M. Inoue, K. Takechi, *Chem. Commun.* **2013**, *49*, 9152 – 9154.
[19] G. Zhao, Z. Xu, K. Sun, *J. Mater. Chem. A* **2013**, *1*, 12862 – 12867.
[20] H.-D. Lim, K.-Y. Park, H. Song, E. Y. Jang, H. Gwon, J. Kim, Y. H. Kim, M. D. Lima, R. O. Robles, X. Lepró, R. H. Baughman, K. Kang, *Adv. Mater.* **2013**, *25*, 1348 – 1352.
[21] W.-M. Liu, T.-T. Gao, Y. Yang, Q. Sun, Z.-W. Fu, *Phys. Chem. Chem. Phys.* **2013**, *15*, 15806 – 15810.
[22] S. Liu, Z. Wang, C. Yu, Z. Zhao, X. Fan, Z. Ling, J. Qiu, *J. Mater. Chem. A* **2013**, *1*, 12033 – 12037.
[23] Z. Guo, D. Zhou, X. Dong, Z. Qiu, Y. Wang, Y. Xia, *Adv. Mater.* **2013**, *25*, 5668 – 5672.
[24] J.-J. Xu, D. Xu, Z.-L. Wang, H.-G. Wang, L.-L. Zhang, X.-B. Zhang, *Angew. Chem.* **2013**, *125*, 3979 – 3982; *Angew. Chem. Int. Ed.* **2013**, *52*, 3887 – 3890.
[25] H.-D. Lim, H. Song, H. Gwon, K.-Y. Park, J. Kim, Y. Bae, H. Kim, S.-K. Jung, T. Kim, Y. H. Kim, X. Lepro, R. Ovalle-Robles, R. H. Baughman, K. Kang, *Energy Environ. Sci.* **2013**, *6*, 3570 – 3575.
[26] G. V. Chase, S. Zecevic, T. W. Wesley, J. Uddin, K. A. Sasaki, P. G. Vincent, V. Bryantsev, M. Blanco, D. D. Addison, US Patent Application No. 20120028137, **2012**.
[27] S. S. Zhang, D. Foster, J. Read, *J. Power Sources* **2010**, *195*, 1235 – 1240.
[28] Y. Shao, F. Ding, J. Xiao, J. Zhang, W. Xu, S. Park, J.-G. Zhang, Y. Wang, J. Liu, *Adv. Funct. Mater.* **2013**, *23*, 987 – 1004.
[29] M. M. Ottakam Thotiyl, S. A. Freunberger, Z. Peng, P. G. Bruce, *J. Am. Chem. Soc.* **2012**, *135*, 494 – 500.
[30] B. D. McCloskey, A. Speidel, R. Scheffler, D. C. Miller, V. Viswanathan, J. S. Hummelshøj, J. K. Nørskov, A. C. Luntz, *J. Phys. Chem. Lett.* **2012**, *3*, 997 – 1001.
[31] H.-D. Lim, K.-Y. Park, H. Gwon, J. Hong, H. Kim, K. Kang, *Chem. Commun.* **2012**, *48*, 8374 – 8376.
[32] R. Black, S. H. Oh, J.-H. Lee, T. Yim, B. Adams, L. F. Nazar, *J. Am. Chem. Soc.* **2012**, *134*, 2902 – 2905.
[33] Y. Chen, F. Li, D.-M. Tang, Z. Jian, C. Liu, D. Golberg, A. Yamada, H. Zhou, *J. Mater. Chem. A* **2013**, *1*, 13076 – 13081.
[34] A. Spadoni, M. Falconieri, M. Lanchi, R. Liberatore, M. Marrocco, G. S. Sau, P. Tarquini, *Int. J. Hydrogen Energy* **2012**, *37*, 1326 – 1334.
[35] H. Greijer, J. Lindgren, A. Hagfeldt, *J. Phys. Chem. B* **2001**, *105*, 6314 – 6320.
[36] C. Laoire, S. Mukerjee, E. J. Plichta, M. A. Hendrickson, K. M. Abraham, *J. Electrochem. Soc.* **2011**, *158*, A302 – A308.
[37] J.-L. Shui, J. S. Okasinski, P. Kenesei, H. A. Dobbs, D. Zhao, J. D. Almer, D.-J. Liu, *Nat. Commun.* **2013**, *4*, 2255.
[38] L. Suo, Y.-S. Hu, H. Li, M. Armand, L. Chen, *Nat. Commun.* **2013**, *4*, 1481 – 1489.

 © 2014 Wiley-VCH Verlag GmbH & Co. KGaA, Weinheim